

Inverse-Designed Silicon Nitride Arbitrary Mode Splitters for Interferometric Optical Sensors

Narges Dalvand,^{1,*} Julian L. Pita Ruiz,¹ and Michaël Ménard¹

¹ Department of Electrical Engineering, École de Technologie Supérieure (ÉTS), Montreal, QC H3C 1K3, Canada

*narges.dalvand.1@ens.etsmtl.ca

Abstract: We demonstrate a compact, freeform silicon nitride device that splits the input fundamental mode between an output fundamental mode and a designated high-order output mode, specified at the design stage, for interferometric sensing applications. © 2025 The Author(s)

Interferometric photonic sensors hold great potential for clinical, chemical, and biological diagnostics [1]. Common types include Mach-Zehnder interferometers, microring resonators, and photonic crystal structures [2]. However, conventional sensors often require large chip areas and exhibit low limited detection sensitivity (LOD). To address these limitations, interferometric sensors based on bimodal waveguides were introduced [3]. These evanescent field sensors rely on interference between the fundamental mode and the first high-order mode of a multimode output waveguide, achieving a detection limit of 2.5×10^{-7} . Since then, several mode splitters have been proposed, including long-period grating couplers using ma-P polymer with power efficiencies of 43 % and 42 % for TE₀₀ and TE₀₂, respectively [4], as well as a shifted junction waveguide that excites TE₀₀ and TE₀₁ with an equal power efficiency of 46 % [5]. However, a compact device on a standard platform that allows the selection of any high-order mode among those supported by the multimode waveguide is still lacking. In this work, we demonstrate a compact silicon nitride (SiN) device with an output multimode waveguide supporting four modes, where the input power is split between the fundamental mode and a high-order mode that can be arbitrarily chosen at the design stage. We believe this work represents a significant contribution to the advancement of interferometric sensors.

The compact device was designed using the fundamental mode of a single mode waveguide as the input mode in the inverse design process, while the fundamental mode and the second-order mode of a multimode waveguide were used as output modes.

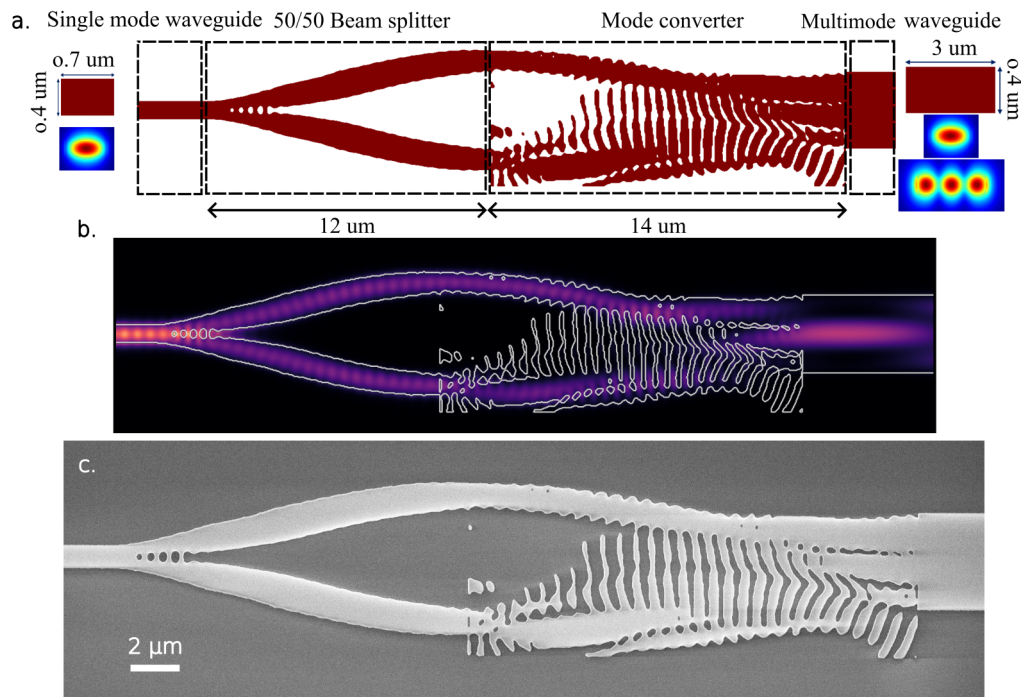


Fig. 1: **Inverse-designed arbitrary mode splitter.** (a) Device design, showing a freeform beam splitter and mode converter. (b) Simulated electric field magnitude at 1550 nm. (c) SEM image of the fabricated device.

The inverse design process was split into two parts to improve the performance of the optimization process. Therefore, two separate processes were conducted: one for designing the beam splitter and another for designing

the mode converter (see Fig. 1a). The beam splitter and mode converter were designed using Lumopt, a Python-based continuous adjoint optimization wrapper. Both of them optimized the response of the device over the C-band for the TE polarization. The 50-50 beam splitter was designed within a rectangular optimization region with a $6\ \mu\text{m} \times 12\ \mu\text{m}$ footprint, whereas the mode converter used a $6\ \mu\text{m} \times 14\ \mu\text{m}$ region. As an initial condition, a Y-branch structure was used for the beam splitter, whereas for the mode converter, two S-bends were used. The beam splitter plays a key role in efficiently guiding the mode conversion, particularly by equalizing the power between the fundamental mode and the high-order mode at the output multimode waveguide. Although the multimode waveguide supports four TE modes, only the TE_{00} and the desired high-order mode are excited simultaneously, and no power is coupled into the other modes. The magnitude of the electric field is shown in Fig. 1b. The device was fabricated by ANT on a SIN platform with a core thickness of 400 nm and top and bottom claddings of 3 μm and 4.5 μm , respectively. An SEM image of the fabricated device is presented in Fig. 1c.

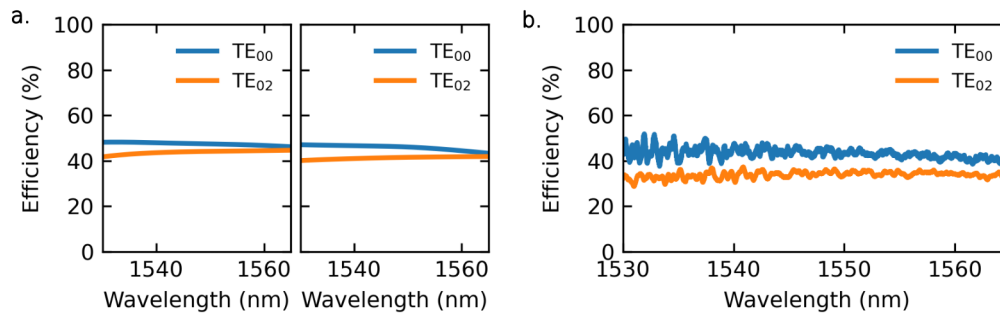


Fig. 2: **Simulation and experimental results for a mode splitter for TE_{00} and TE_{02} .** (a) Efficiency of TE_{00} and TE_{02} for an ideal device (left) and power efficiency of the device under a lateral overetching of approximately 14 nm (right). (b) Experimental results of the fabricated device.

Fig. 2a shows the simulated results for the fundamental mode and the second high-order mode in the C-band for a mode splitter optimized with a minimum feature size of 120 nm. The left subfigure represents the ideal design, whereas the right subfigure illustrates the simulated efficiency when the device is affected by a lateral overetch of 14 nm. The results indicate a simulated efficiency of 47% for TE_{00} and 44% for TE_{02} at 1550 nm in the ideal design. For the device affected by a 14-nm overetch, the higher-order mode is more sensitive to fabrication variations than the fundamental mode, as the efficiency of TE_{02} decreases to 42% at 1550 nm, while TE_{00} remains at 47% (see Fig. 2a, right). Notably, incorporating a shifted junction between the single-mode input and multimode output waveguides can enhance both the efficiency and power ratio of the device. Fig. 2b presents the experimental results. The efficiency of the fundamental mode is approximately 43%. However, as observed in the fabrication variation simulation, the higher-order mode is more sensitive to fabrication errors, exhibiting a 9% lower efficiency than the simulated value, with a measured efficiency of 35%. This discrepancy suggests that the fabricated device may have been affected by more complex variations than those accounted for in the simulations.

In summary, the results demonstrate the effectiveness of the inverse-designed mode splitter in achieving high efficiency for both fundamental and higher-order modes. This technique allows us to select the desired high-order mode to enhance the sensitivity of the sensor application.

Acknowledgments

The authors would like to thank the National Science and Engineering Research Council of Canada (NSEC), PRIMA Québec, and AEPONYX for their financial support. The support of CMC Microsystems to access fabrication resources is also appreciated.

References

1. J. C. Ramirez, L. M. Lechuga, L. H. Gabrielli, and H. E. Hernandez-Figueroa, "Study of a low-cost trimodal polymer waveguide for interferometric optical biosensors," *Optics express*, vol. 23, no. 9, pp. 11 985–11 994, 2015.
2. M. C. Estevez, M. Alvarez, and L. M. Lechuga, "Integrated optical devices for lab-on-a-chip biosensing applications," *Laser & Photonics Reviews*, vol. 6, no. 4, pp. 463–487, 2012.
3. K. E. Zinoviev, A. B. González-Guerrero, C. Domínguez, and L. M. Lechuga, "Integrated bimodal waveguide interferometric biosensor for label-free analysis," *Journal of lightwave technology*, vol. 29, no. 13, pp. 1926–1930, 2011.
4. Y. Liang, M. Zhao, Z. Wu, and G. Morthier, "Investigation of grating-assisted trimodal interferometer biosensors based on a polymer platform," *Sensors*, vol. 18, no. 5, p. 1502, 2018.
5. J. Haines, P. U. Naik, K. Ji, V. Vitali, Y. Franz, P. Petropoulos, and M. Guasoni, "Subwavelength and broadband on-chip mode splitting with shifted junctions," *Optics Express*, vol. 32, no. 14, pp. 24 072–24 080, 2024.